

FIR filter design for GNSS-synchronized clock

Hongwei Wu, Duo Li, and Sihong Gu

Abstract—We investigate a scheme that utilizes the one-pulse-per-second (1PPS) signal of a Global Navigation Satellite System (GNSS) receiver as a reference to synchronize the local clock in the time synchronization system. The noise of the correct signal caused by jitter in the 1PPS signal is the main factor affecting the synchronization precise. To reduce the noise and improve the synchronization precise, a finite-impulse-response filter is proposed based on least-squares estimation and moving average. The experimental results indicate that the noise can be effectively reduced with this filter. The proposed scheme helps in realizing a synchronized clock for which the one-second precision-time-protocol (PTP) variance is improved by two orders of magnitude and the kilo-second PTP variance is improved by one order of magnitude over those of GNSS receivers.

Keywords—Finite-impulse-response filter, least-squares estimation, clock synchronization, Global Navigation Satellite System, chip scale atomic clock

I. INTRODUCTION

TIME synchronization plays an essential role in navigation, target tracking, power grid monitor, digital communication networks, and wireless sensor networks [1]–[4]. Global Navigation Satellite System (GNSS) satellites transfer accurate time, thus enabling the receivers on Earth to generate high-accuracy one-pulse-per-second (1PPS) signals. The 1PPS signal output of the GNSS receiver is widely used as the time scale to realize time synchronizations. However, the error of 1PPS signal provided by the GNSS receiver is commonly of the order of a few tens of nanoseconds mainly caused by jitter noise. Therefore, when the 1PPS signal is used directly as a time scale for the time synchronization system, the precision in time synchronization might not meet the precision requirements for certain applications [5].

Many solutions have been proposed to improve the precision. One alternative but well-known approach is synchronizing the local clock, which is precise but not accurate, to the 1PPS signal, which is accurate but not precise [6]. The GNSS-synchronized clock combines the advantages of both the local clock and GNSS receiver thereby achieving high-accuracy and high-precision synchronization. The basic block diagram of a GNSS-synchronized clock used for this study is shown in Figure 1. The time error of the local clock is measured with a high-resolution time-interval-error (TIE) counter where the 1PPS signal output of the GNSS receiver is used as a reference. The measurement, also termed the correct signal, is then processed by a filter to suppress noise. The phase shifting

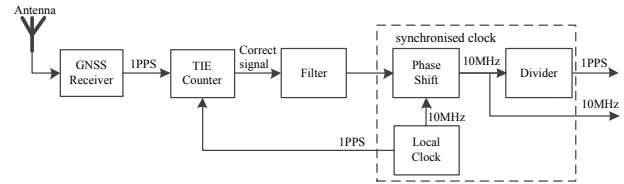


Fig. 1. Basic block diagram of a GNSS-synchronized clock.

circuit next eliminates the time error of the local clock using the processed correct signal to produce a high-accuracy and high-precision 1PPS signal. This signal can then be used as a time scale to realize time synchronization.

The filter is used to reduce the noise of the correct signal that is mainly induced by the jitter of the 1PPS signal output of the GNSS receiver thereby improving the accuracy of synchronization. The Kalman filter is generally used to suppress noise [7]. Its performance though declines when the noise is not Gaussian [8]. An alternative is the finite-impulse-response (FIR) filter [6], which handles noise of arbitrary distribution [9]. We propose a FIR filter based on the principle of least-squares estimation and moving average for which a second-order polynomial model of a clock time error is used. We also present a phase (time) shifting circuit configured on a field programmable gate array (FPGA) to eliminate the time error.

This paper is organized into four sections, where apart from the introduction in Section I, Section II outlines the proposed FIR filter. Section III presents a phase shifting circuit configured on a FPGA. Section IV presents the experimental validation. Lastly, the concluding are provided in Section V.

II. FIR FILTER

Let $y(t)$ denotes the normalized frequency deviation of a local clock. A typical mathematical expression for $y(t)$ is [10]

$$y(t) = b_1 + b_2 t + \varepsilon(t), \quad (1)$$

where the quantities b_1 and b_2 are the initial frequency deviation and the linear frequency drift, and $\varepsilon(t)$ is a generic random component describing the clock noise. The integral of $y(t)$ is the time error $x(t)$ given by [11]

$$x(t) = b_0 + b_1 t + \frac{b_2}{2} t^2 + w(t), \quad (2)$$

where b_0 is the initial time error and $w(t)$ is the integral of $\varepsilon(t)$. We assume the time error of the clock is measured each second. From Eq. (2), the time error $x(n)$ at the n th second is then

$$x(n) = b_0 + b_1 n + \frac{b_2}{2} n^2 + w(n), \quad (3)$$

where $n = 0, 1, 2, \dots$. The correct signal, which is the relative time difference between the 1PPS signal output of the GNSS

This work was supported by the National Key R&D Program of China under Grant 2017YFB0503200.

Hongwei Wu is with the University of Chinese Academy of Sciences, Beijing 100049, China, e-mail:hwwu@wipm.ac.cn.

Duo Li is with the University of Chinese Academy of Sciences, Beijing 100049, China.

Sihong Gu is with Wuhan Institute of Physics and Mathematics, Chinese Academy of Sciences, Wuhan Hubei 430071, China.

Manuscript received 2018;

receiver and the local clock, is given by

$$z(n) = x(n) + v(n), \quad (4)$$

where $v(n)$ denotes the noise component primarily associated with the 1PPS of the receiver. Typically, the root mean square value of $w(n)$ is of order of a few hundred picoseconds whereas the root mean square value of $v(n)$ is of order of a few tens of nanoseconds. That is, $\langle w^2(n) \rangle \ll \langle v^2(n) \rangle$ and therefore $w(n)$ can be neglected in Eq. (3) and Eq. (4), thereby becoming, respectively,

$$x(n) = b_0 + b_1 n + \frac{b_2}{2} n^2, \quad (5)$$

$$z(n) = b_0 + b_1 n + \frac{b_2}{2} n^2 + v(n), \quad (6)$$

For this study, $z(n)$ is processed by a FIR filter to suppress the noise component $v(n)$. Thereby the processed correct signal $\hat{x}(n)$ is obtained from

$$\hat{x}(n) = \sum_{i=0}^{N-1} h(i)z(n-i), \quad (7)$$

where $h(i)$ is the coefficient of FIR filter. If we neglect the uncertainty in the phase shifting module, the local clock timing is corrected with $\hat{x}(n)$, and the time error for the synchronized local clock is then given by

$$x_o(n) = x(n) - \hat{x}(n), \quad (8)$$

where $x_o(n)$ is the time error of synchronized clock. Eq. (7) and Eq. (8) indicate that the function of the FIR filter is to get the optimal estimate of $x(n)$ from $\{z(n-N+1), z(n-N+2) \cdots z(n)\}$. We use the least-squares estimation and moving average to design the FIR filter based on this principle.

Extended to matrix form, Eq. (5) and Eq. (6) become

$$\mathbf{x} = \mathbf{A}\mathbf{b}, \quad (9)$$

$$\mathbf{z} = \mathbf{A}\mathbf{b} + \mathbf{v}, \quad (10)$$

where $\mathbf{x} = [x(n) \ x(n-1) \ \cdots \ x(n-N+1)]^T$, $\mathbf{b} = [b_0 \ b_1 \ b_2]^T$, \mathbf{A} is given by:

$$\mathbf{A} = \begin{bmatrix} 1 & n & n^2/2 \\ 1 & n-1 & (n-1)^2/2 \\ \cdots & \cdots & \cdots \\ 1 & n-N+1 & (n-N+1)^2/2 \end{bmatrix}, \quad (11)$$

\mathbf{z} and \mathbf{v} by, respectively,

$$\mathbf{z} = [z(n) \ z(n-1) \ \cdots \ z(n-N+1)]^T, \quad (12)$$

$$\mathbf{v} = [v(n) \ v(n-1) \ \cdots \ v(n-N+1)]^T, \quad (13)$$

Our goal is to obtain an optimal estimate of $x(n)$ from the data sequence $\{z(n-N+1), z(n-N+2) \cdots z(n)\}$. From regression analysis, the least-squares estimate of \mathbf{x} involves finding a coefficient $\hat{\mathbf{b}}$ such that:

$$F(\hat{\mathbf{b}}) = \min_{\mathbf{b}} \{F(\mathbf{b})\} \quad (14)$$

where

$$F(\mathbf{b}) = (\mathbf{z} - \mathbf{A}\mathbf{b})^T (\mathbf{z} - \mathbf{A}\mathbf{b}), \quad (15)$$

We can then obtain the least-squares estimate $\hat{\mathbf{x}}$ from $\hat{\mathbf{x}} = \mathbf{A}\hat{\mathbf{b}}$. The derivative of $F(\mathbf{b})$ with respect \mathbf{b} is

$$F'(\mathbf{b}) = \frac{\partial F(\mathbf{b})}{\partial \mathbf{b}} = 2(\mathbf{A}^T \mathbf{A}\mathbf{b})^T - 2(\mathbf{A}^T \mathbf{z})^T, \quad (16)$$

When $F'(\mathbf{b}) = 0$, $F(\mathbf{b})$ is minimum. Hence $\hat{\mathbf{b}}$ is given by:

$$\hat{\mathbf{b}} = (\mathbf{A}^T \mathbf{A})^{-1} (\mathbf{A}^T \mathbf{z}), \quad (17)$$

and therefore, the least-squares estimate is

$$\hat{\mathbf{x}} = \mathbf{A}\hat{\mathbf{b}} = \mathbf{A}(\mathbf{A}^T \mathbf{A})^{-1} (\mathbf{A}^T \mathbf{z}), \quad (18)$$

Substituting Eq. (11) and Eq. (12) into Eq. (18) and making a transformation, we get the desired $\hat{x}(n)$, which is an element of $\hat{\mathbf{x}}$; specifically,

$$\hat{x}(n) = \sum_{j=0}^{N-1} g(j)z(n-j), \quad (19)$$

where

$$g(j) = \frac{3(3N^2 - 3N + 2) - 18(2N - 1)j + 30j^2}{N(N+1)(N+2)}, \quad (20)$$

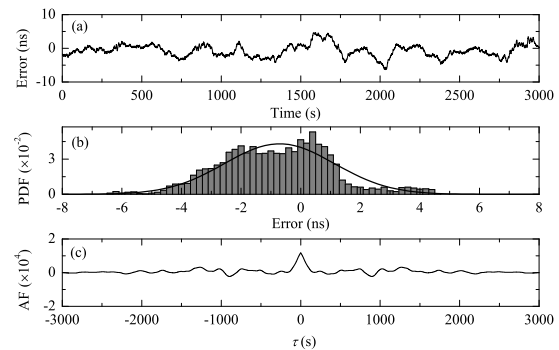


Fig. 2. Characteristics of the estimate error with the least-squares estimation obtained from simulations: (a) estimate error, (b) normalised columnar distribution of the error, where the solid line is the probability density curve for a standard Gaussian distribution, and (c) autocorrelation function of the error. PDF: Probability Density Function. AF: Autocorrelation Function, τ : Time difference of the autocorrelation function. Simulation parameter settings: $b_0 = 0$, $b_1 = 5 \times 10^{-11}$, $b_2 = 1.15 \times 10^{-16}$, stability of local clock = $2 \times 10^{-10} \tau^{-1/2}$, $N = 400$, $\text{std.}(v(n)) = 10$ ns.

From Eq. (19) and Eq. (20), we obtain by simulations $\hat{x}(n)$, which is the least-squares estimate of $x(n)$ from the data sequence $\{z(n-N+1), z(n-N+2) \cdots z(n)\}$. The estimate error is shown in Figure 2(a). Figure 2(b, c) demonstrates that the estimate error follows approximately an independent random Gaussian distribution. As moving averages are suitable for smoothing such errors, we applied this method to smooth $\hat{x}(n)$,

$$\tilde{\hat{x}}(n) = \frac{1}{M} \sum_{i=0}^{M-1} \hat{x}(n-i) = \sum_{i=0}^{M-1} \sum_{j=0}^{N-1} \frac{1}{M} g(j)z(n-i-j), \quad (21)$$

Let $L - 1 = N + M - 2$, Eq. (21) can be transformed to

$$\tilde{x}(n) = \sum_{i=0}^{L-1} h(i)z(n-i), \quad (22)$$

where $h(i)$ is given by:

$$\text{when } M \leq N, h(i) = \begin{cases} \frac{1}{M} \sum_{j=0}^i g(j) & 0 \leq i \leq M-1 \\ \frac{1}{M} \sum_{j=i-M+1}^i g(j) & M \leq i \leq N-1 \\ \frac{1}{M} \sum_{j=1}^{L-i} g(N-j) & N \leq i \leq L-1 \end{cases}, \quad (23)$$

$$\text{when } M > N, h(i) = \begin{cases} \frac{1}{M} \sum_{j=0}^i g(j) & 0 \leq i \leq N-1 \\ \frac{1}{M} & N \leq i \leq M-1 \\ \frac{1}{M} \sum_{j=1}^{L-i} g(N-j) & M \leq i \leq L-1 \end{cases}, \quad (24)$$

Hence, for our synchronization scheme, Eq. (22) is the expression for the FIR filter with Eq. (23) and Eq. (24) giving the coefficients of filter.

III. PHASE SHIFT MODULE

A phase (time) shifting circuit configured on a FPGA is described that eliminates the time error of the local clock with the processed correct signal. The 1PPS signal provided to the node in the distributed system is obtained by dividing up the 10-MHz frequency signal; changing the control word phase-shifts the 1PPS signal. By this means, the minimum step in phase shifting of the 1PPS signal is 100 ns. Shifting the phase of the 10-MHz frequency signal before division provides a finer shift in the 1PPS signal. We use a phase locked loop (PLL) within the Cyclone III EP3C25E144C8N FPGA to achieve this phase shifting of the 10 MHz frequency signal. The PLL architecture is shown in Figure 3. The output frequency of the PLL is

$$f_{in} = \frac{M \times N}{N \times K} = \frac{f_{vco}}{K}, \quad (25)$$

where f_{in} is the input frequency, f_{vco} the voltage-controlled oscillator (VCO) frequency, M the feedback multiplier counter, N the pre-divider counter, and K the post-divider counter. The PLL can generate eight phases of the voltage-

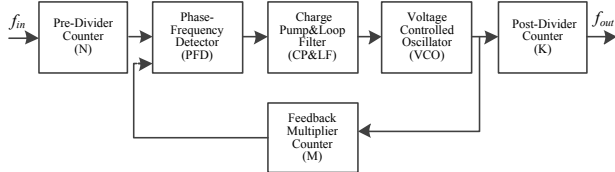


Fig. 3. A typical PLL architecture

controlled oscillator (VCO); see Figure 4 [12]. Fine-resolution phase shifting is implemented by allowing the post-divider counter to use any of the eight phases of the VCO as a

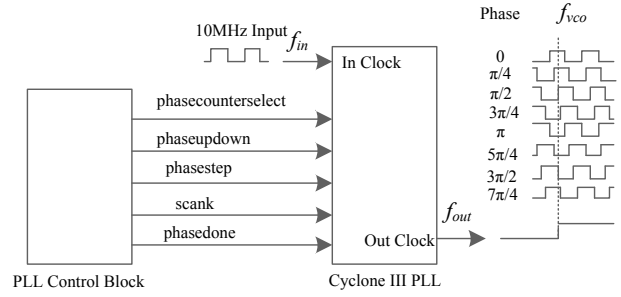


Fig. 4. Example of Cyclone III PLL phase-shift control

reference clock. This allows to shift the phase of f_{in} with fine resolution with

$$\delta T = \frac{T_{vco}}{8}, \quad (26)$$

An experiment was performed to investigate the phase shifting performance achieved by the above method. In the experiment with the input frequency set at 10 MHz, $N = 1$, $M = 10$, and $K = 10$, the VCO frequency is then 1000 MHz and the output clock frequency is 10 MHz. According to Eq. (26), the minimum phase shifting is 125 ps. In the experiment, a set of phase adjustments was performed at 400 s intervals. Each set performed 20 dynamic phase shifts (each one yielding a 125-ps phase shift). The experimental results are shown in Figure 5(a). The phase of the output clock remains stable when the phase is not adjusted but changes when the phase is adjusted. Using the average value of the data on the same "platform" [Figure 5(a)] as the phase value of the output clock, the relationship between phase and the number of phase shifts can be obtained [Figure 5(b)]. The average for the fine resolution of the phase shift is 125.0583 ps.

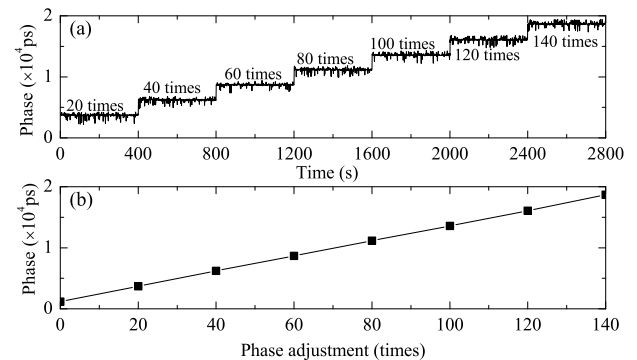


Fig. 5. Dependence of phase shift with (a) time and (b) phase adjustments.

IV. RESULTS AND ANALYSIS

Currently, oscillators are generally used as local clocks to implement time synchronization. The frequency drift of an oscillator is high, and frequent corrections are required to ensure precision in synchronization within the allowable range. Nevertheless, the correct interval is too short to be implemented when a rigorous synchronization is required. The frequency drift of atomic clock is more than two orders of magnitude lower than that of an oscillator, which can greatly

increase the correct interval. Therefore, a Rb atomic clock is used when a rigorous synchronization is required. The chip scale atomic clock (CSAC) is a new type of atomic clock that is compact and has a power consumption at least two orders of magnitude lower than that of a Rb atomic clock. It also operates with low frequency drift. In the experiment, we used the CSAC developed in-house as our local clock the volume being 19 cm^3 , a power consumption of 180 mW, a frequency stability of $2 \times 10^{-10} \tau^{-1/2}$, and a day frequency drift of 1×10^{-11} . The frequency drift of the CSAC is more than two orders of magnitude below that of an oscillator with the same volume and power consumption. The GNSS receiver used in the experiment is a Motorola M12M TIMING, and the TIE counter is a TDC-GP21 produced by ACAM; $z(n)$ is obtained by the TIE counter for the GNSS receiver. Simultaneously, to obtain a reference, $z_H(n)$ is obtained by the counter for the Hydrogen atomic clock (CH-75A). $x(n)$ is equal to $z_H(n)$ as the accuracy and stability of the Hydrogen atomic clock is more than one order of magnitude higher than those of an CSAC. The noise of the unprocessed correct signal is then obtained from $z(n) - z_H(n)$ [Figure 6(a)], with a root mean square error of about 10.13 ns. Figure 6(b) shows the power spectrum of the unprocessed correct signal. Figure 6(b, c) demonstrates that the noise is not strictly Gaussian.

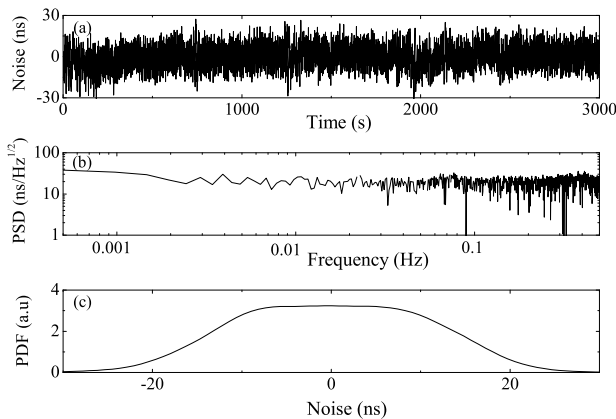


Fig. 6. (a) Noise of the unprocessed correct signal, root mean square error being about 10.13, (b) power spectrum of the noise, and (c) normalised probability density of the noise. PSD: Power Spectral Density, PDF: Probability Density Function..

A FIR filter was designed with specifications matching Equation (22), where $N = 70$ and $M = 500$, and taking into consideration resources and performance. Figure 7 indicates that, using a commercially available low-cost GNSS receiver, the FIR filter attains equal precision as an expensive Hydrogen atomic clock .

We also designed a Kalman filter according to the method proposed in [13]. Using both the FIR and Kalman filters to perform filtering on $z(n)$, separately, the noise of the processed correct signals were obtained for comparison (Figure 8). The root mean square error of the noise is reduced to 0.98 ns by the FIR filter but only to 2.33 ns by the Kalman filter. When presented non-Gaussian noise, the former suppresses the noise more effectively than the latter.

The one-second precision-time-protocol (PTP) variance of

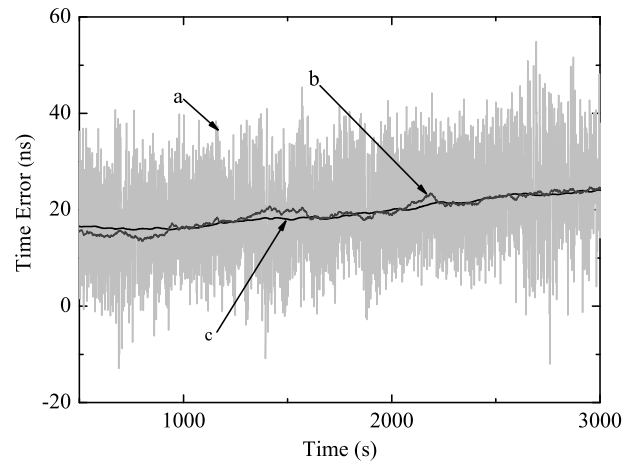


Fig. 7. Time errors associated with a: the unprocessed correct signal with a GNSS receiver, b: the unprocessed correct signal with the Hydrogen atomic clock, and c: the processed correct signal with the FIR filter.

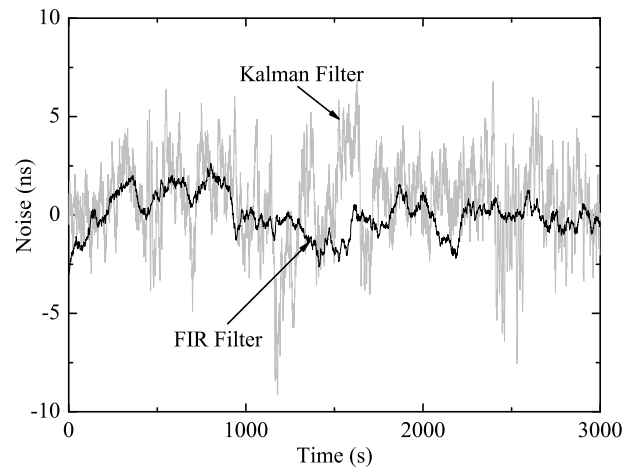


Fig. 8. Noise of the processed correct signal with the different filters.

the GNSS receiver used in this study is 1.12×10^{-8} ; the kilo-second variance is 1.02×10^{-8} . For the synchronized clock implemented with the FIR filter, the one-second PTP variance is 1.37×10^{-10} and the kilo-second variance is 1.06×10^{-9} . With the FIR filter, the one-second PTP variance is better by two orders of magnitude and the thousand-second PTP variance is better by one order of magnitude compared with the GNSS receiver.

V. CONCLUSION

Using the second-order polynomial model for a local clock time error and the principle of least-squares estimation and moving average, we designed a FIR filter to process the correct signal output of the TIE counter; the noise of the correct signal was effectively suppressed. We also compared the capability of the FIR and Kalman filters to suppress noise when presented with non-Gaussian noise. The experimental results show that: 1) non-Gaussian noise is contained in the noise components of the correct signal output of the TIE counter; and 2) the noise of the processed correct signal with the FIR filter is lower than that with the Kalman filter. The experimental results indicate

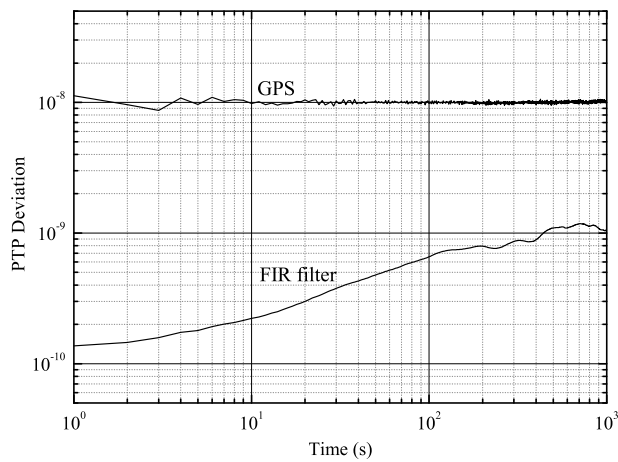


Fig. 9. Precision-time-protocol (PTP) variance of time synchronized chip scale atomic clock.

that the FIR filter designed is better than the Kalman filter when non-Gaussian noise is present. The proposed scheme described in this paper helps to produce a synchronized clock that achieves two orders of magnitude improvement of the one-second PTP variance and one order of magnitude improvement of the thousand-second PTP variance over those of a GNSS receiver.

REFERENCES

- [1] F. Gong, and M. L. Sichitiu, On the Accuracy of Pairwise Time Synchronization *IEEE Transactions on Wireless Communications* **16** (2017) 2664-2677.
- [2] L. Lin, J. Zhang, M. Ma, and H. Yan, Time Synchronization for Molecular Communication with Drift, *IEEE Communications Letters* **21** (2017) 476-479.
- [3] J. H. Cho, H. Kim, and S. Wang, A Novel Method for Providing Precise Time Synchronization in a Distributed Control System Using Boundary Clock *IEEE Trans. Instrum. Meas* **58** (2009) 2824-2829.
- [4] L. Zhan, Y. Liu, W. Yao, J. Zhao, and Y. Liu, Utilization of Chip-Scale Atomic Clock for Synchronphasor Measurements *IEEE Trans. Power Deliv.* **31** (2016) 2299-2300.
- [5] W. Wang, Noise Suppression in GPS-Disciplined Frequency Synchronization system *Fluct. Noise Lett.* **45** (2011) 303-313.
- [6] L. Arceo-Miquel, Y. S. Shmaliy, and Ibarra- O. Manzano, Optimal Synchronization of Local Clocks by GPS 1PPS Signals Using Predictive FIR Filters *IEEE Trans. Instrum. Meas* **58** (2009) 1833-1840.
- [7] L. Galleani, and P. Tavella., On the Use of the Kalman Filter in Timescales *Metrologia* **40** (2003) 326-334.
- [8] R. Fitzgerald, Divergence of the Kalman Filter *IEEE Trans. Autom. Control* **16** (1971) 736-747.
- [9] T.W. Parks, and C.S. Burrus, Digital filter design ,Wiley-Interscience 1987.
- [10] P. Tavella, Statistical and Mathematical Tools for Atomic Clocks *Metrologia* **45** (2008) 183-192.
- [11] L. Galleani, and P. Tavella, Detection of Atomic Clock Frequency Jumps with the Kalman Filter *IEEE Trans. Ultrason. Ferroelectr. Freq. Control* **59** (2012) 504-509.
- [12] Altera Corporation, A Cyclone III Device Handbook, Available: https://www.altera.com.cn/content/dam/altera-www/global/en_US/pdfs/literature/hb/cyc3/cyclone3_handbook.pdf (2012).
- [13] Y. S. Shmaliy, An unbiased FIR filter for TIE model of a local clock in applications to GPS-based timekeeping *IEEE Trans. Ultrason. Ferroelectr. Freq. Control* **53** (2006) 2664-2677.